Ferredoxin:NADP(H) Oxidoreductase Abundance and Location Influences Redox Poise and Stress Tolerance[1]

Marina Kozuleva, Tatjana Goss, Manuel Twachtmann, Katherina Rudi, Jennifer Trapka, Jennifer Selinski, Boris Ivanov, Prashanth Garapati, Heinz-Juergen Steinhoff, Toshiharu Hase, Renate Scheibe, Johann P. Klare, and Guy T. Hanke*

Institute of Basic Biological Problems, Russian Academy of Sciences, Puschino, 142290 Russia (M.K., B.I.); Department of Plant Physiology (T.G., M.T., J.T., J.S., P.G., R.S., G.T.H.) and Department of Biophysics (K.R., H.-J.S., J.P.K.), Osnabrück University, Osnabrück 49076, Germany; Institute for Protein Research, Osaka University, Osaka 565-0871, Japan (T.H.); and School of Biochemistry and Chemistry, Queen Mary University of London, London E1 4NS, United Kingdom (G.T.H.)

ORCID IDs: 0000-0002-0763-5389 (P.G.); 0000-0002-5888-0157 (H.-J.S.); 0000-0002-0631-3900 (T.H.); 0000-0002-6140-6181 (R.S.); 0000-0002-5761-5968 (J.P.K.); 0000-0002-6167-926X (G.T.H.).

In linear photosynthetic electron transport, ferredoxin:NADP(H) oxidoreductase (FNR) transfers electrons from ferredoxin (Fd) to $NADP^+$. Both NADPH and reduced Fd (Fd^{red}) are required for reductive assimilation and light/dark activation/deactivation of enzymes. FNR is therefore a hub, connecting photosynthetic electron transport to chloroplast redox metabolism. A correlation between FNR content and tolerance to oxidative stress is well established, although the precise mechanism remains unclear. We investigated the impact of altered FNR content and localization on electron transport and superoxide radical evolution in isolated thylakoids, and probed resulting changes in redox homeostasis, expression of oxidative stress markers, and tolerance to high light in planta. Our data indicate that the ratio of Fd^{red} to FNR is critical, with either too much or too little FNR potentially leading to increased superoxide production, and perception of oxidative stress at the level of gene transcription. In FNR overexpressing plants, which show more NADP(H) and glutathione pools, improved tolerance to high-light stress indicates that disturbance of chloroplast redox poise and increased free radical generation may help "prime" the plant and induce protective mechanisms. In *fnr1* knock-outs, the NADP(H) and glutathione pools are more oxidized relative to the wild type, and the photoprotective effect is absent despite perception of oxidative stress at the level of gene transcription.

In photosynthetic electron transport (PET), electrons are accepted at PSI by ferredoxin (Fd), before being transferred to the flavo-enzyme ferredoxin:NADP(H) oxidoreductase (FNR). PSI, Fd, and FNR are reported to be present at a 1:5:3 ratio in spinach chloroplasts (Böhme, 1978). Very high control coefficients of FNR for photosynthesis of 0.94 (at saturating light) and 0.7 (at limiting light) were calculated from a study on antisense tobacco (*Nicotiana tabacum*) plants with variable FNR concentrations (Hajirezaei et al., 2002). In higher plants, FNR enzymes have a dynamic relationship with the membrane, being recruited to various membrane complexes (Andersen et al., 1992; Jose Quiles and Cuello, 1998; Zhang et al., 2001), including the two dedicated FNR-tethering proteins Tic62 (Benz et al., 2009) and TROL (Jurić et al., 2009). Interaction of FNR with Tic62 and TROL is dependent on the LiR1 protein (Yang et al., 2016) and is regulated by pH (Alte et al., 2010; Lintala et al., 2014). The catalytic cycle of FNR is well described (Batie and Kamin, 1981, 1984, 1986; Carrillo and Ceccarelli, 2003; Cassan et al., 2005), with two reduced Fd (Fd^{red}) molecules binding in sequence to reduce the flavin cofactor before reduction of one $NADP^+$. There is strong evidence for formation of a ternary complex (Martinez-Júlvez et al., 2009).

During light excitation, the PET chain is a rich source of reactive oxygen species (ROS). Superoxide radical ($O_2^{\bullet-}$) produced mainly at PSI (Allen and Hall, 1974), and singlet oxygen ($^1O_2$) produced at PSII (Telfer et al., 1994) are the dominant species evolved. Due to the damaging nature of ROS, very efficient scavenging (or antioxidant) mechanisms exist in chloroplasts to prevent oxidative damage: $^1O_2$ can be quenched by β-carotene, α-tocopherol, or plastoquinone (Krieger-Liszkay et al., 2008), while in the water-water cycle (Asada, 1999) $O_2^{\bullet-}$ is rapidly converted to H_2O_2 by superoxide dismutase (SOD) enzymes or plastoquinol (Mubarakshina and Ivanov, 2010). H_2O_2 can be

[1] This work was supported by the Deutsche Forschungsgeneinschaft through funding of Project 2 in the Collaborative Research Center (SFB) 944 at the University of Osnabrück. M.K. was supported by grant HA 5921/2-1 for the initiation of international collaboration.

* Address correspondence to g.hanke@qmul.ac.uk.

The author responsible for distribution of materials integral to the findings presented in this article in accordance with the policy described in the Instructions for Authors (www.plantphysiol.org) is: Guy T. Hanke (g.hanke@qmul.ac.uk).

G.T.H., M.K., J.P.K., T.H., and R.S. conceived the original research plan; G.T.H., T.H., R.S., H.-J.S., and J.K. supervised the experiments; G.T.H., T.G., M.K., J.P.K., and K.R. performed most of the experiments; M.T., P.G., and J.S. performed some of the experiments; M.K., G.T.H., and J.P.K. analyzed most of the data; G.T.H. wrote the article with contributions from all the authors.

www.plantphysiol.org/cgi/doi/10.1104/pp.16.01084

converted to the highly damaging $OH^{\bullet}$ radical in the Fenton reaction by any of the multiple iron, copper, or manganese centers in the thylakoid membrane or free ions (Snyrychová et al., 2006). To prevent this, the chloroplast is rich in proteins that reductively convert H_2O_2 to H_2O, such as peroxiredoxin, which can be reduced by either thioredoxin (König et al., 2002) or the NADPH-dependent thioredoxin reductase C (Pulido et al., 2010), and other peroxidase enzymes, which use ascorbate as the electron donor (Mittler et al., 2004; Foyer and Noctor, 2011). Ascorbate can be directly regenerated using photosynthetic electrons via Fd^{red} (Asada, 1999). Alternatively, dehydroascorbate reductase can reduce ascorbate using reduced glutathione (GSH). In the chloroplast, the oxidized glutathione (GSSG) is rereduced by the glutathione reductase (GR) 2 enzyme (Chew et al., 2003) using NADPH. It is now well established that retrograde signaling from the chloroplast controls gene expression and that oxidative species contribute to this signaling pathway (Mittler et al., 2004; Oelze et al., 2008; Mubarakshina Borisova et al., 2012). A balance therefore exists between rapid removal of damaging oxidative species and maintenance of appropriate concentrations necessary to initiate signaling cascades. A simplified diagram showing the interconnections between FNR, the ($Fd^{red}/Fd + e^{-}$), and ($NADPH/NADP^{+} + H^{+} + 2e^{-}$) redox couples and redox homeostasis is shown in Figure 1.

In addition to its classical role in photosynthesis, there is a well-established connection between FNR and oxidative stress. This was first discovered in *Escherichia coli*, where the equivalent (though nonphotosynthetic) protein was found to be a diaphorase of the $O_2^{\bullet-}$ generator methyl viologen (MV) and was also identified as a member of the stress-responsive *soxRS* regulon (Liochev et al., 1994). Overexpression of FNR in *E. coli* caused an upregulated *soxRS* response, and mutants lacking FNR were found to be more susceptible to MV-mediated oxidative stress, although the *soxRS* response was not affected (Krapp et al., 2002). Furthermore, it was discovered that higher plant FNR was capable of rescuing mutants of the *E. coli* gene (Krapp et al., 1997). It was suggested that FNR could act to balance the NADPH redox poise, thus affecting expression of the *soxRS* regulon. Alternative mechanisms by which FNR could promote tolerance to oxidative stress include potentially transferring electrons from NADPH to scavengers of ROS, acting in the repair of iron centers, or even by functioning as an antioxidant itself (Krapp et al., 1997; Krapp et al., 2002; Giró et al., 2006).

An analogous connection to the stress response was discovered for higher plant FNR in work on antisense of tobacco *FNR*, which showed decreased chlorophyll, carotenoids, and photosynthetic capacity and increased lipid peroxidation and membrane leakage upon high-light treatment (Palatnik et al., 2003). Staining of whole leaves for ROS indicated that acceptor limitation at PSI caused an increased reduction state of the electron transport chain and $^1O_2$ production. In addition, overexpression of pea (*Pisum sativum*) FNR in tobacco has been shown to afford protection from oxidative stress (Rodriguez et al., 2007). When subjected to MV-mediated oxidative stress, the overexpressing plants showed less membrane leakage, chlorophyll loss, and damage to PSII than the wild type. Mirroring the work on tobacco, it has been reported that single mutants of both Arabidopsis (*Arabidopsis thaliana*) genes, *FNR1* and *FNR2*, show increased membrane leakage when challenged with MV (Lintala et al., 2009). In the same study the authors found an isoform-specific effect, with *fnr2* knock-downs proving more tolerant than wild-type or *fnr1* knock-outs to high-light stress at low temperatures. In *fnr2* knock-downs, the remaining FNR1 is membrane bound, while in *fnr1* mutants all remaining FNR2 is soluble. Intriguingly, there is other evidence for a relationship between FNR location within the chloroplast and oxidative stress. In tobacco, MV-derived, PET-dependent oxidative stress causes the solubilization of FNR (Palatnik et al., 1997), and it was recently reported that chloroplasts from Arabidopsis *trol* mutants, which lack one of the FNR-thylakoid tethering proteins, generate lower

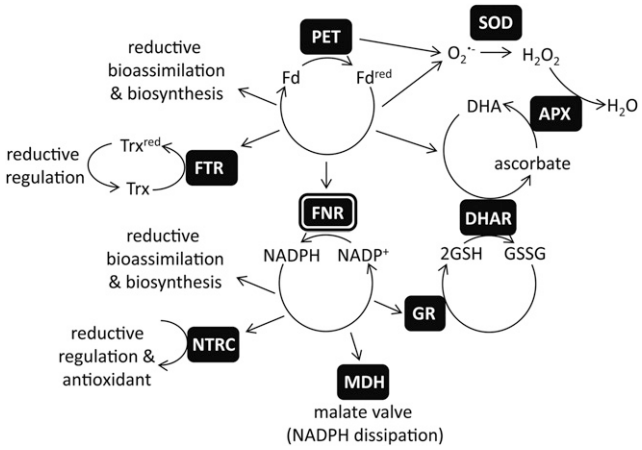

Figure 1. FNR plays a central role in chloroplast redox metabolism. Simplified diagram of chloroplast redox metabolism related to the transfer of electrons between the Fd redox couple ($Fd^{red}/Fd + e^{-}$) and the NADP(H) redox couple ($NADPH/NADP^{+} + H^{+} + 2e^{-}$) by the enzyme FNR. PET reduces Fd to Fd^{red}, and both PET and Fd^{red} are sources of $O_2^{\bullet-}$. There are many Fd-dependent enzymes, including essential components of bioassimilation and biosynthesis (Hanke and Mulo, 2013) and the Fd:thioredoxin reductase (FTR), which reduces thioredoxin (Trx), transducing a redox signal to regulate many chloroplast enzymes (Schürmann and Buchanan, 2008). The majority of Fd^{red} is oxidized by the enzyme FNR to reduce $NADP^{+}$ to NADPH. $NADP^{+}$ is regenerated by many enzymes, including other proteins involved in biosynthesis and bioassimilation and the NADPH-dependent Trx reductase C, which also reduces thiol groups, resulting in a redox signal and supports antioxidant metabolism by regenerating 2-Cys peroxiredoxin (Dietz et al., 2002). When the redox poise of the NADP(H) pool is too reduced, $NADP^{+}$ can be regenerated by the NADP-MDH and operation of the malate valve to export reducing equivalents from the chloroplast (Backhausen et al., 1994). The $O_2^{\bullet-}$ radical is removed in the water-water cycle by the action of first SOD and then ascorbate peroxidase (APX), resulting in oxidation of ascorbate to dehydroascorbate (Foyer and Halliwell, 1976; Groden and Beck, 1979; Asada, 1999). Reductive regeneration of ascorbate can be supported directly by Fd^{red}, or through GSH oxidation to GSSG by dehydroascorbate reductase (DHAR). GSH regeneration is supported in turn by NADPH, through action of GR. Thus, both Fd^{red} and FNR are involved in removal of ROS.

amounts of superoxide than wild type upon illumination (Vojta et al., 2015).

We previously generated Arabidopsis plants with increased FNR by overexpressing genes for different maize (*Zea mays*) FNR proteins under control of the native Arabidopsis promoter (Twachtmann et al., 2012). We used ZmFNR3, which is predominantly soluble, and ZmFNR1, which can bind to the thylakoid membrane when expressed in Arabidopsis. This resulted in FNR contents 1.5 to 2 times that of the wild type. These enzymes have nearly identical catalytic properties (Okutani et al., 2005) that are similar to those of the native Arabidopsis FNR (Hanke et al., 2005), meaning that the major difference between overexpression of Zm*FNR1* and Zm*FNR3* lies in the chloroplast localization of the introduced enzymes. To better understand the impact of FNR content and location on plant stress tolerance, we have compared $NADP^+$ and glutathione redox poise, $O_2^{\bullet-}$ generation and responsive genes, and high-light stress response in plants expressing Zm*FNR1* and Zm*FNR3* and *fnr1* mutants, which lack membrane-bound FNR. Our data provide evidence that the content and location of FNR affect the redox balance of the chloroplast, with knock-on effects on redox signaling and stress tolerance.

RESULTS

FNR Content Correlates with Redox Poise of the NADP(H) Pool

To understand how FNR abundance and localization in Arabidopsis affects $NADP^+$ photoreduction and to examine the downstream effects of this, we first selected two genotypes with extreme differences in FNR content and location. In Arabidopsis *fnr1* mutants, no FNR remains bound to the thylakoid (Lintala et al., 2007; Hanke et al., 2008), and overexpression of maize *FNR1* (Zm*FNR1*) in Arabidopsis results in enhanced accumulation of FNR at the thylakoid, specifically at TROL-dependent complexes (Twachtmann et al., 2012). Total FNR activity of the thylakoids from these genotypes confirms this (Fig. 2A). While there is no difference in total electron flux by thylakoids from wild type, *fnr1*, and Zm*FNR1*-expressing plants (Fig. 2B), the difference in FNR contents translate into decreased $NADP^+$ photoreduction capacity of *fnr1* thylakoids and increased $NADP^+$ photoreduction capacity in thylakoids from Zm*FNR1* plants (Fig. 2C). This is in agreement with work on FNR-overexpressing tobacco, where a 20% stimulation of $NADP^+$ photoreduction in isolated thylakoids was measured (Rodriguez et al., 2007), indicating that membrane-bound FNR can photoreduce $NADP^+$. In the wild type, rates of electron flux to $NADP^+$ (Fig. 2C) are about one-third to one-half the capacity for total electron flux from H_2O (Fig. 2B). This suggest that either loosely bound or soluble FNR lost in thylakoid preparation might be required for maximum rates of electron flow to $NADP^+$ or that FNR capacity limits flux to $NADP^+$, as suggested by the antisense work in tobacco (Hajirezaei et al., 2002).

We then tested whether the redox poise of NADP(H) [the $NADP^+$/NADP(H) ratio] reflects the thylakoid capacity for $NADP^+$ photoreduction. The redox state of the chloroplast NADP(H) pool is very accurately reflected in the activation state of the NADP-malate dehydrogenase (NADP-MDH; Scheibe and Stitt, 1988), reductive activation of which is strongly inhibited by $NADP^+$. We therefore compared steady-state activity to total capacity (Fig. 2D) to determine the activation state of NADP-MDH (Fig. 2E) in plants with altered FNR contents. This experiment showed significantly lower NADP-MDH activation in *fnr1* plants and significantly elevated NADP-MDH activation state in Zm*FNR1* plants, confirming that redox poise of the NADP(H) pool does indeed correlate with the $NADP^+$ photoreduction capacity of the thylakoids. This also demonstrates that in Arabidopsis, the abundance and activity of NADP-MDH is regulated to partly counteract the change in $NADP^+$ photoreduction capacity. These data are in good agreement with work on tobacco FNR-antisense plants showing that the $NADP^+$/NADPH ratio is increased (Hajirezaei et al., 2002). It also confirms the findings of Lintala et al. (2014), who showed that in *tic62/trol* double mutant plants lacking both FNR-membrane tethers, $NADP^+$/NADPH ratios were increased and the activation state of NADP-MDH decreased (Lintala et al., 2014), indicating that FNR localization is critical to $NADP^+$ redox poise.

FNR Contents Correlate with Glutathione Redox State

Altered NADP(H) redox poise likely impacts on the redox state of the entire chloroplast, and we therefore investigated redox poising mechanisms in plants with altered FNR content. GR reduction of glutathione (GSSG to 2× GSH) in the chloroplast is dependent on NADPH (Mittler et al., 2004; Foyer and Noctor, 2011). We investigated the impact of FNR content and location on total and oxidized amounts of glutathione in plant leaves. In this experiment, we also examined the impact of FNR localization in more detail: in addition to Zm*FNR1*-expressing plants, plants expressing Zm*FNR3*, which is nearly all soluble (Twachtmann et al., 2012), were analyzed. Both total and oxidized leaf glutathione are significantly elevated in the *fnr1* mutant (Fig. 3A), and the redox poise of glutathione is more oxidized (Fig. 3B). Expression of both maize FNR genes results in a decrease in total glutathione (Fig. 3A) and in the proportion of GSSG (Fig. 3B). This is statistically significant only in the Zm*FNR1*-expressing lines, indicating that membrane-bound FNR might affect glutathione reduction more strongly than soluble FNR.

Thylakoid-Bound FNR Activity Decreases $O_2^{\bullet-}$ Production in the Light

In the reduced state, Fd is capable of electron donation to O_2, generating $O_2^{\bullet-}$ (Misra and Fridovich, 1971),

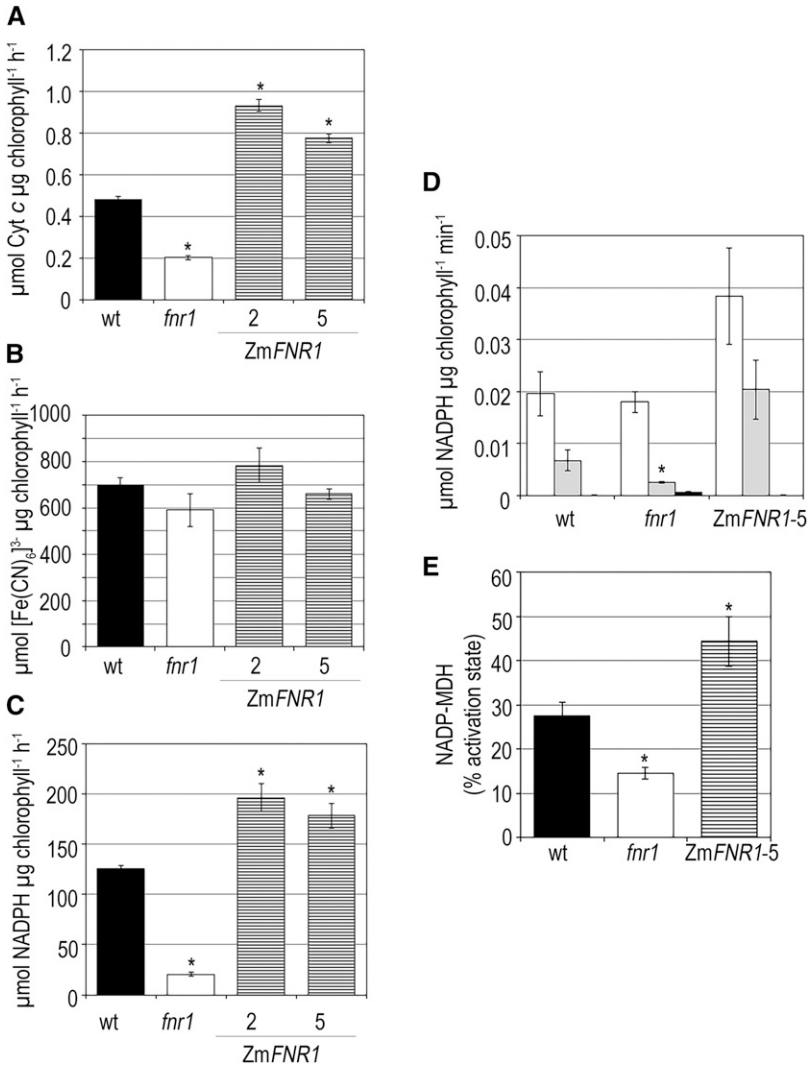

Figure 2. FNR activity and chloroplast NADP(H) poise is altered in FNR transgenics. A, FNR activity of isolated thylakoid membranes from Arabidopsis wild type, *fnr1* mutant, and two independent lines expressing maize *FNR1*, measured as reduction of cytochrome *c* on addition of NADPH and 10 μM Fd. B, Capacity for light-dependent electron flux from H_2O by isolated thylakoid membranes of the indicated plants, measured as reduction of $[Fe(CN)_6]^{3-}$ by PSI on illumination. C, Light-dependent $NADP^+$ photoreduction by isolated thylakoid membranes from the indicated plants, measured as reduction of $NADP^+$ by PSI on illumination. A, B, and C values are means ± SE of three measurements and typical of two separate experiments. D, Measurement of NADP(H) redox poise. Arabidopsis plants with the indicated genotypes were harvested either under growth-light (gray) or dark-adapted (black) conditions. Extracts were used for measurement of steady-state NADP-MDH activity. Total enzyme activity (white bars) was determined following incubation of the extract for 40 min in activating buffer (see Methods). Values are means ± SE of three to six biological replicates. As dark values are low to nondetectable, original values are given in Supplemental Table S1 for clarity. E, Percentage activation state of NADP-MDH in the indicated genotypes under steady-state growth-light conditions, calculated for the individuals averaged in part D. Values are means ± SE of three to six biological replicates. Significant differences in *fnr1*- and *FNR1*-expressing plants from the wild type in a *t* test for small samples are indicated by $*P < 0.05$.

and inefficient Fd oxidation might lead to longer lifetimes for Fd^{red} and greater $O_2^{\bullet-}$ production. To test this hypothesis, we measured light-dependent $O_2^{\bullet-}$ production by thylakoid membranes (identical to those used in Fig. 2) using electron paramagnetic resonance (EPR). This semi-in vitro system was used because intact chloroplasts contain SOD, which has an extremely high rate constant of $O_2^{\bullet-}$ dismutation, complicating accurate quantitation of $O_2^{\bullet-}$. The PET chain was reconstituted by addition of Fd and $NADP^+$. Figure 4, A and B, show light-dependent thylakoid $O_2^{\bullet-}$ generation using the $O_2^{\bullet-}$ detector 1-hydroxy-4-isobutyramido-2,2,6,6-tetramethylpiperidinium, which can react with $O_2^{\bullet-}$ in both soluble and membrane phases (Kozuleva et al., 2011; Kozuleva et al., 2015). Addition of SOD to the suspension, eliminating soluble $O_2^{\bullet-}$, allowed dissection of free radical generation by membrane-bound and soluble pathways.

Figure 4B shows that when Fd is added to illuminated membranes there is a significant increase in soluble $O_2^{\bullet-}$ production, as the number of reduced FeS centers at the acceptor side of PSI increases. The further addition of saturating concentrations of $NADP^+$ caused a significant decrease in soluble $O_2^{\bullet-}$ generation. Intermembrane $O_2^{\bullet-}$ production, presumably resulting from O_2 reduction by phyllosemiquinone at PSI (Kozuleva et al., 2014), was unaffected by addition of FNR substrates. This finding is consistent with previous work on illuminated pea thylakoids (Kozuleva and Ivanov, 2010) where $NADP^+$ suppressed O_2 reduction by Fd, but not by membrane-bound components.

We then examined $O_2^{\bullet-}$ production in thylakoids isolated from different genotypes (Fig. 4C). For comparison, the experiment presented in Figure 4C used the same thylakoids as the electron transport measurements in Figure 2. As expected, the addition of $NADP^+$ to *fnr1* thylakoids had very little impact on $O_2^{\bullet-}$ generation from Fd^{red} in the light. In planta, *fnr1* chloroplasts will contain alternative sinks for Fd^{red}, including soluble native FNR (AtFNR2), and this will presumably alleviate $O_2^{\bullet-}$ production by electron transfer to $NADP^+$ from Fd^{red} to some extent. Total rates of $O_2^{\bullet-}$ generation from Zm*FNR1*

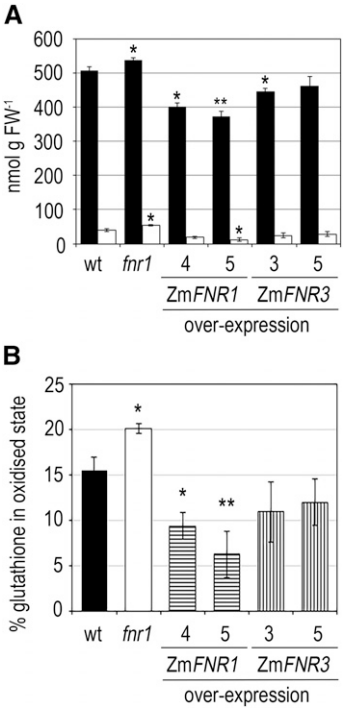

Figure 3. Downstream impact of FNR content on redox poise of glutathione. A, Measurement of total glutathione (black) and glutathione in the oxidized state (white) in leaves of wild type, *fnr1*, two independent lines expressing Zm*FNR1*, and two independent lines expressing Zm*FNR3*, measured by enzymatic cycling assay. B, Percentage of glutathione in the oxidized state in leaves of wild type, *fnr1*, two independent lines expressing Zm*FNR1*, and two independent lines expressing Zm*FNR3*, calculated from the data shown in A. Values are means ± SE of three to six biological replicates. In comparison with wild type, statistical significance in a *t* test for small samples is indicated by $*P < 0.05$, $**P < 0.01$.

thylakoids in the presence of $NADP^+$ are lower than in the wild type, probably due to a shorter lifetime of Fd^{red}, and therefore decreased rates of $O_2^{\bullet-}$ generation from Fd^{red}. This correlates with the higher rate of $NADP^+$ photoreduction by Zm*FNR1* thylakoids (Fig. 2).

Excess Soluble FNR Increases $O_2^{\bullet-}$ Production in the Light

The data in Figure 4C indicate that membrane-bound FNR is capable of quenching $O_2^{\bullet-}$ production by decreasing the dwell-time of electrons on Fd and passing electrons to stromal sinks. To test whether the addition of soluble FNR could compensate for the loss of membrane-bound FNR in *fnr1* thylakoids, we challenged the thylakoid $O_2^{\bullet-}$ detection system with soluble FNR. We previously calculated that maize chloroplasts contain approximately 30 μM FNR in the combined soluble and membrane fractions (Okutani et al., 2005). In Arabidopsis, the proportion of soluble FNR is between 25% and 50% in wild-type plants (Hanke et al., 2005; Benz et al., 2009). We therefore added a soluble, recombinant ZmFNR3 concentration of approximately the same order (5 μM) to *fnr1* thylakoids and illuminated in the presence and absence of $NADP^+$ (Fig. 5). Surprisingly, addition of soluble FNR to the system resulted in a dramatic increase in $O_2^{\bullet-}$ production, and this was partly ameliorated by the omission of $NADP^+$.

Altered FNR Content Impacts on ROS and Redox Perception by the Plant

It is well documented that signals originating from both glutathione redox poise and $O_2^{\bullet-}$ influence gene expression (Mehta et al., 1992; Wagner et al., 2004; Mhamdi et al., 2010). To determine whether the FNR-dependent changes to in vitro free radical generation (Figs. 4 and 5) also occur in planta, we tested transcript abundance of classical markers responding to general and $O_2^{\bullet-}$-specific oxidative stress (*At2g21640* and *DIR5*, respectively; Mehterov et al., 2012) and chloroplast redox poise (*NADP-MDH*; Scheibe et al., 2005; Hameister et al., 2007) by real time quantitative RT-PCR (qRT-PCR). In addition, we selected genes that could potentially be connected to both FNR and redox poise, by interrogating databases of microarray and RNAseq data (see Supplemental Table S2 for details). We selected five genes that are up-regulated in arrays comparing *fnr1* mutants with wild type, which also showed up-regulation in conditions expected to impact on redox metabolism: *WRKY53*, *WRKY70*, *LEA5/SAG21*, *ACD6*, and *SYP122*. Transcript abundance of these genes was compared between wild type, the *fnr1* mutant, and two lines each overexpressing Zm*FNR1* and Zm*FNR3*, respectively, by qRT-PCR (Fig. 6). The two stress marker genes (*DIR5* and *At2g21640*) and *NADP-MDH* have wild-type expression levels in *fnr1*. Apart from *ACD6*, transcripts of all genes potentially responding to both *FNR* loss and ROS or redox perturbation are increased in *fnr1*, although only *SAG21* and *SYP122* are statistically significant. FNR-overexpressing plants also showed increased expression of these genes, although the amplitude of this change varies between lines. In contrast to *fnr1*, markers for both general and $O_2^{\bullet-}$-specific oxidative stress are also upregulated in the overexpressors.

Finally, *NADP-MDH* transcripts were significantly increased in all Zm*FNR*-overexpressing lines, consistent with its role in the malate valve, exporting reducing equivalents to the cytosol when the $NADP^+$/NADPH poise is excessively reduced (Scheibe, 2004). Although the correlation between FNR content and activation state of NADP-MDH is consistent between Arabidopsis (Fig. 2) and tobacco (Hajirezaei et al., 2002), this is not the case for total enzyme capacity. FNR overexpression in tobacco has no impact, while in tobacco *fnr* antisense lines, NADP-MDH activity increases (Scheibe and Dietz, 2012). By contrast, in Arabidopsis we found that knock-out of 50% FNR had no effect on total NADP-MDH activity, while overexpression of FNR leads to an increased NADP-MDH transcript (Fig. 4). Total activity also increases on FNR overexpression, but this is not

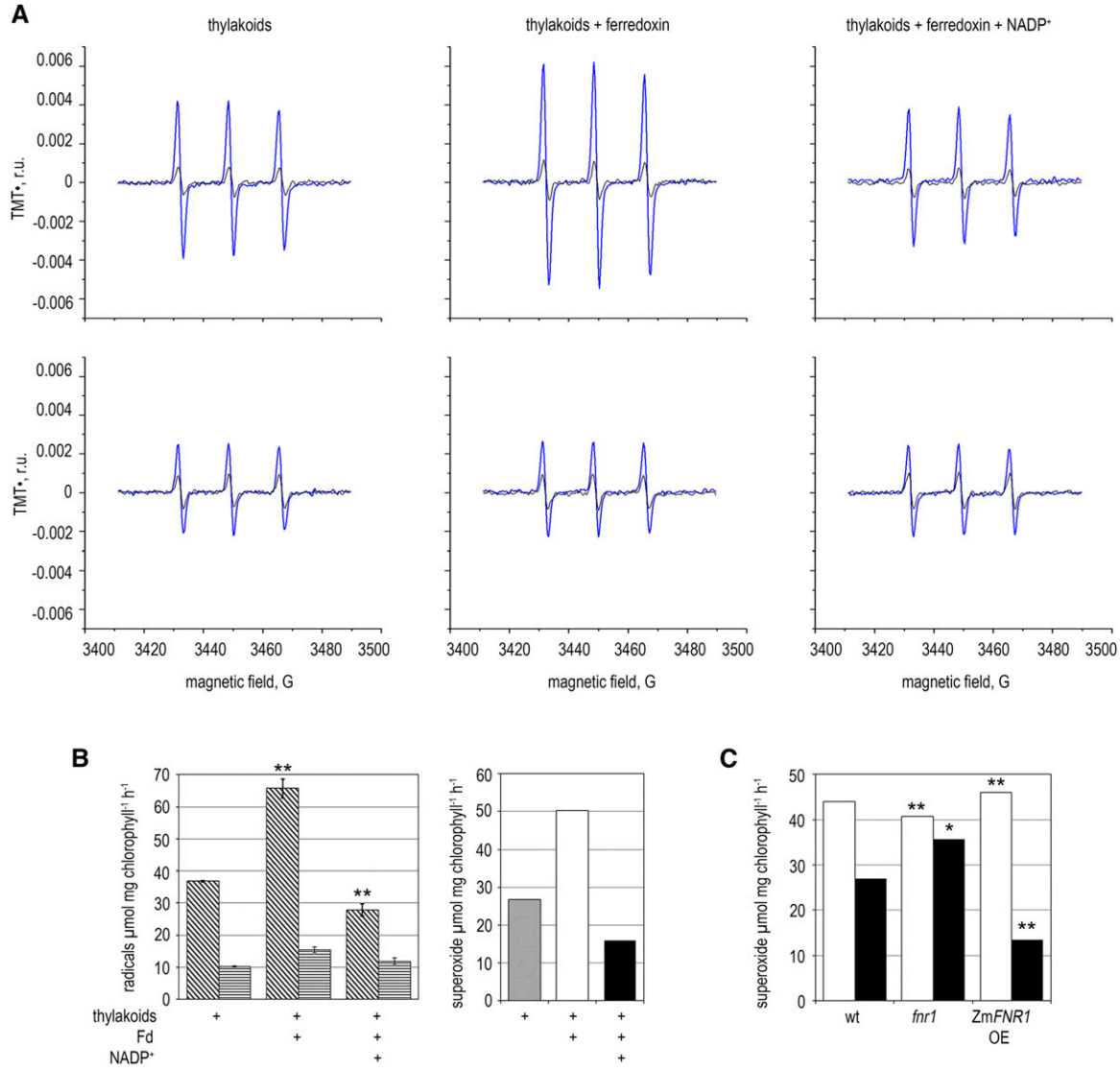

Figure 4. Impact of thylakoid FNR content on $O_2^{\bullet-}$ production. A, Detection of light-dependent $O_2^{\bullet-}$ evolution from purified Arabidopsis thylakoid membranes. Representative EPR spectra before (black lines) and after (blue lines) illumination. The experiment was performed in the absence (top panels) and presence (bottom panels) of SOD to remove soluble $O_2^{\bullet-}$. B, Left, light-dependent $TMT^{\bullet}$ radical generation by thylakoid membranes, calculated using the spectra shown in part A and two further replicates, in the absence (diagonal stripes) and presence (horizontal stripes) of SOD. In comparisons between −SOD measurements, significant difference from thylakoid-only measurements in a *t* test for small samples is indicated by $*P < 0.05$, $**P < 0.01$. Right, light-dependent soluble $O_2^{\bullet-}$ evolution by Arabidopsis thylakoid membranes calculated by subtracting +SOD from the −SOD rates shown in the graph on the left. C, Light-dependent soluble $O_2^{\bullet-}$ evolution in thylakoid membranes from the indicated Arabidopsis genotypes, calculated by subtracting the +SOD from the −SOD rates in the presence of Fd (white bars) or Fd and $NADP^+$ (black bars). SD of the original data were less than 5% and significant difference from the equivalent wild-type measurement in a *t* test for small samples is indicated by $*P < 0.05$, $**P < 0.01$. Experiment was repeated two times with similar results.

statistically significant (Fig. 2). The reasons for this difference between species are unclear, but the signals leading to up-regulation of the NADP-MDH gene are poorly understood. Results in *fnr* antisense tobacco were interpreted as a response to an excessively reduced stroma (Scheibe and Dietz, 2012), and it may be that relative light intensity or photoperiod play a role. Indeed, transcript and protein of the single copy NADP-MDH gene in Arabidopsis only increase in response to high light when plants are grown in short-day, but not long-day conditions (Becker et al., 2006). No consistent difference in transcripts was observed between Zm*FNR1*- and Zm*FNR3*-expressing lines. In general, stronger responses were seen in Zm*FNR1-2* and Zm*FNR3-3* than in Zm*FNR1-5* and Zm*FNR3-5*.

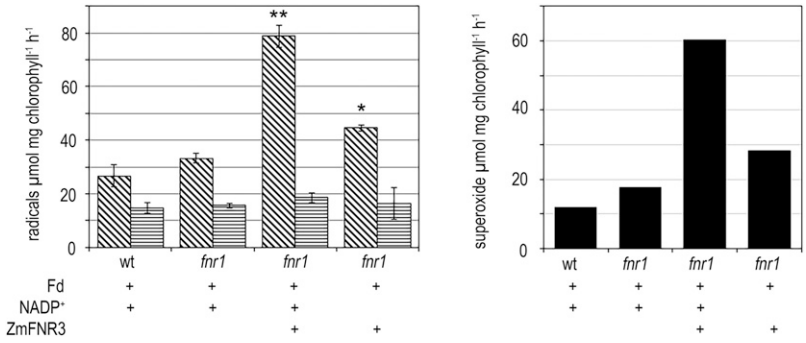

Figure 5. Impact of additional soluble FNR on superoxide production. Left, light-dependent $TMT^{\bullet}$ radical generation by *fnr1* thylakoid membranes illuminated with variable combinations of Fd, $NADP^+$, and soluble FNR in the absence (diagonal stripes) and presence (horizontal stripes) of SOD. In comparisons between −SOD measurements, statistical difference from *fnr1* + Fd + $NADP^+$ in a *t* test for small samples is indicated by $*P < 0.05$, $**P < 0.01$. Right, light-dependent soluble $O_2^{\bullet-}$ evolution in Arabidopsis thylakoid membranes, calculated by subtracting +SOD from the −SOD rates shown in the graph on the left. The experiment was repeated two times with similar results.

There are several reports correlating FNR content with tolerance to high light and other oxidative stresses (Palatnik et al., 2003; Rodriguez et al., 2007; Lintala et al., 2012), and data in Figures 4, 5, and 6 indicate that increasing or decreasing FNR content alters ROS production and perception. We therefore compared the high-light susceptibility of genotypes with altered FNR abundance and location (Fig. 7). In this experiment, high-light treatment of the *fnr1* mutant did not result in significantly more membrane damage (measured as ion leakage) or damage to PSII (measured as ΦII), which is a major site of $O_2^{\bullet-}$ action (Krieger-Liszkay et al., 2011). By contrast, both lines expressing Zm*FNR1* appear partially protected, with significantly less PSII damage and membrane leakage, especially after a short, 1.5-h illumination. This protective effect is less pronounced for Zm*FNR3*-expressing plants, with only ΦII being significantly improved relative to the wild type.

DISCUSSION

Data presented in this study show that changes in FNR abundance and localization produce at least two distinct outcomes that are potentially relevant to plant stress tolerance. Firstly, the efficiency of $NADP^+$ photoreduction has an impact on electron supply to ROS removal pathways. Secondly, altered free radical production, caused by either decreased or increased FNR, can induce changes in gene transcription related to stress tolerance.

A Long Fd^{red} Half-Life Could Result in $O_2^{\bullet-}$ Production

Figure 1 highlights the role of FNR in connecting the (Fd^{red}/Fd + e^-) and ($NADPH/NADP^+ + H^+ + 2e^-$) redox couples. In vitro, uncoupling these pools leads to a longer half-life for Fd^{red}, resulting in increased $O_2^{\bullet-}$ production (*fnr1* in Fig. 4). However, under steady-state conditions, we did not detect up-regulation of specifically $O_2^{\bullet-}$ responsive genes in *fnr1* (Fig. 4), and staining for ROS in the tobacco knock-downs detected a specific increase in $^1O_2$ but not $O_2^{\bullet-}$ (Palatnik et al., 2003). Therefore, under steady-state conditions, other electron acceptors probably quench $O_2^{\bullet-}$ generation from Fd^{red}. Despite this, a prolonged Fd^{red} half-life might be expected in specific conditions, and it is known that plants drastically decrease Fd contents under various stresses (Giró et al., 2006; Tognetti et al., 2006; Liu et al., 2013). Data in Figure 4 indicate that this could be because it is preferable to have charge recombination within PSI than low turnover of Fd^{red}. Indeed, Arabidopsis mutants lacking the main Fd iso-protein, Fd2, are more tolerant of extended high-light treatment (Liu et al., 2013). The authors attribute this to increased photosynthetic cyclic electron flow, but decreased $O_2^{\bullet-}$ production could also play a role. In our experiments, we did not detect greater susceptibility of Arabidopsis *fnr1* mutants to high-light stress (Fig. 7), but Lintala et al. (2009) found that both *fnr1* mutants and *fnr2* knock-downs were more susceptible to MV-induced oxidative stress at room temperature. Decreased FNR is also known to increase susceptibility to photo-oxidative stress in tobacco (Palatnik et al., 2003).

Increased Soluble FNR Results in $O_2^{\bullet-}$ Production

By contrast, increased membrane-bound FNR in the thylakoid system appears to improve coupling between the Fd:Fd^{red} and $NADP^+$:NADPH pools, with less flux to $O_2^{\bullet-}$ in the presence of a $NADP^+$ sink in vitro (Fig. 4), and a more reduced NADP(H) pool (Fig. 2), leading to a more reduced glutathione pool in planta (Fig. 3). Zm*FNR1* plants and, to a lesser extent, Zm*FNR3* plants appear to be more tolerant to high-light treatment (Fig. 7), in line with previous work in tobacco (Rodriguez et al., 2007). Surprisingly, when we attempted to rescue $O_2^{\bullet-}$ production in *fnr1* thylakoids by the addition of

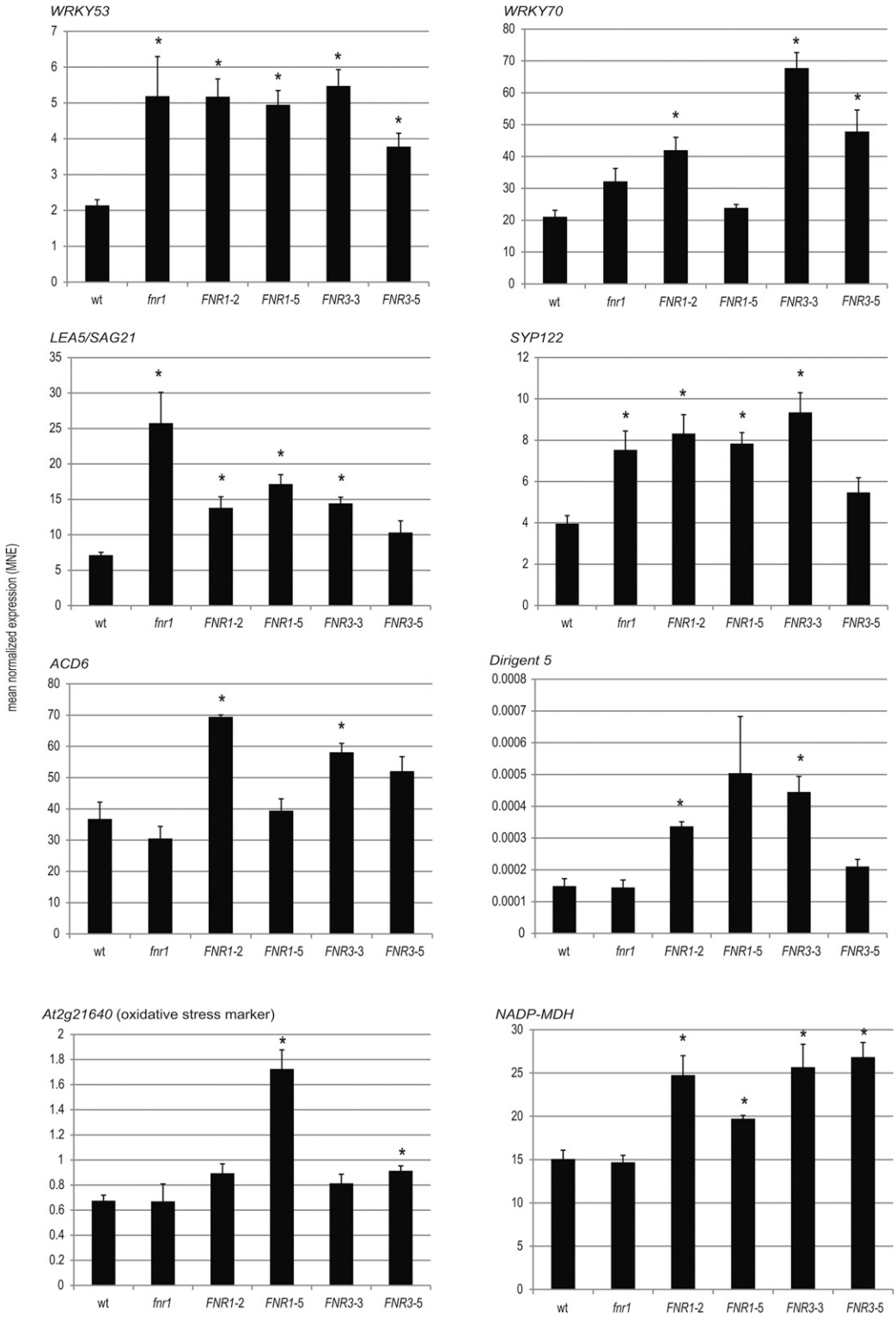

Figure 6. Transcript abundance of ROS and redox responsive genes in wild type, *fnr1*, and two independent lines expressing either membrane bound (Zm*FNR1*) or soluble (Zm*FNR3*) FNR. Genes are: a responsive marker for $O_2^{\bullet -}$, *DIR5*; a responsive marker for oxidative stress, *At2g21640*; a marker for disturbed NADP(H) poise, *NADP-MDH*; and five genes whose transcript is reported to be up-regulated both in *fnr1* and in response to ROS or redox perturbation: *WRKY53, WRKY70, SAG21*, *SYP122*, and *ACD6*. Histograms show mean normalized expression (MNE) relative to the housekeeping gene RAN3. RNA was isolated from plants 3 h into the light period in standard growth conditions, and qRT-PCR was performed with the resulting cDNA. Values are means ± SE of three biological replicates. Statistical significance, in a *t* test is indicated by $*P < 0.05$.

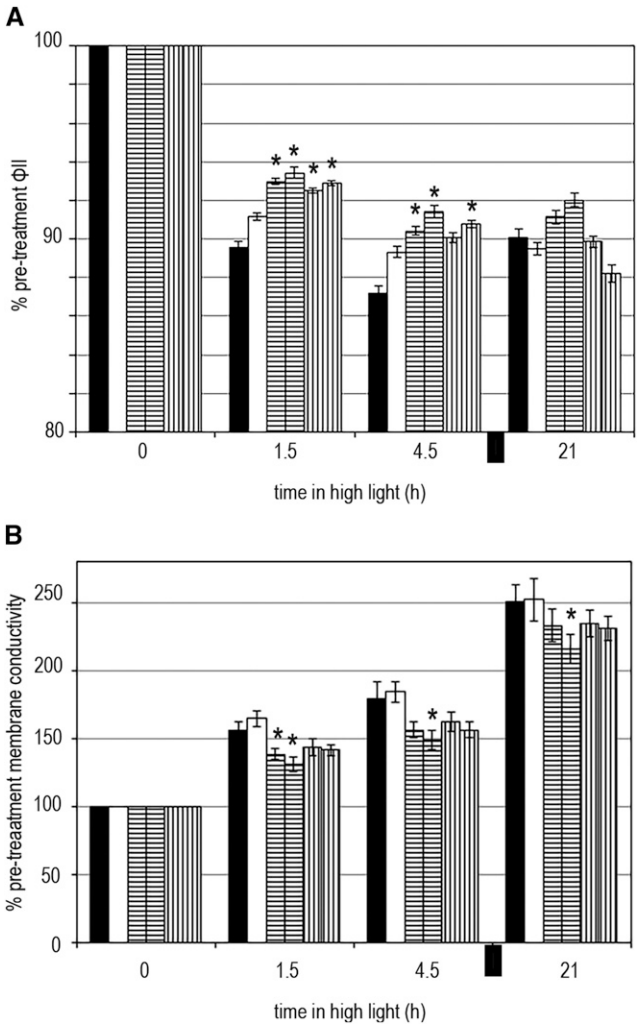

Figure 7. High-light tolerance of *fnr1*- and *FNR*-overexpressing transgenic plants. High light induced damage to wild type (black bars), *fnr1* (white bars), two independent lines overexpressing the membrane-bound Zm*FNR1* (horizontal bars), and two independent lines overexpressing the soluble Zm*FNR3* vertical bars). Leaf discs were excised from the leaves of at least five individual plants 1 h into the light period, floated on 3 mL MilliQ water, and exposed to 600 μE high-light stress. Damage was followed by A, measuring PSII capacity (Φ II of the leaf discs) and B, membrane leakage (increased conductivity of the MilliQ water) at the indicated time points. The dark bar between 4.5 and 21 h represents an 8-h-night period. Data displayed are percent of initial values from five biological replicates, averages of which are given in Supplemental Figure S1. In comparison with changes in the wild type, statistical significance in a *t* test for small samples is indicated by $^*P < 0.05$.

soluble FNR, we measured a dramatic increase in $O_2^{\bullet-}$ evolution (Fig. 5). Interestingly, other studies on illuminated thylakoids report that addition of several flavoenzymes, including FNR, cause an increase in O_2 consumption (Goetze and Carpentier, 1993; Miyake et al., 1998). Although monodehydroascorbate reductase was identified as the most efficient $O_2^{\bullet-}$ catalyst, FNR showed one-half the maximum rate at approximately 1.5 μM enzyme concentrations, still well below the total FNR concentration estimated for the chloroplast of approximately 30 μM (Okutani et al., 2005). Miyake et al. (1998) also report that this activity was independent of Fd, implying that FNR received electrons directly from PSI. By contrast, we measured maximum rates of $O_2^{\bullet-}$ formation in the presence of $NADP^+$, indicating turnover of the enzyme contributes. There are two possible explanations for this result. Firstly, we cannot discount the possibility that excess FNR catalyzes backflow of electrons from photo-NADPH to Fd, which in turn reduces O_2, during the sampling and EPR measurement time. However, this seems unlikely, because the higher FNR content of Zm*FNR1* thylakoids does not drive greater $O_2^{\bullet-}$ production (Fig. 4C).

Alternatively, $O_2^{\bullet-}$ may be generated at FNR. In our system, PSI:Fd:FNR is altered from the in vivo ratio of 1:5:3 (Böhme, 1978). To minimize shading, we used 33 μg chlorophyll mL^{-1}, and assuming a chlorophyll: PSI ratio of 600:1 (Kohorn et al., 1992), this gives a PSI: Fd:FNR of approximately 1:80:80. Under these conditions, one Fd^{red} will pass an electron to one FNR, forming a semiquinone on the FAD until a second Fd^{red} allows completion of the catalytic cycle and reduction of $NADP^+$. Limited electron supply from PSI would therefore extend the lifetime of this unstable semiquinone before the second reduction, leading to increased electron donation to O_2 from the semiquinone. Production of $O_2^{\bullet-}$ by the FAD semiquinone radical of FNR is supported by a study from Bes et al. (1995), who report that while FNR is a poor electron donor to O_2 when the FAD is fully reduced by NADPH, cross-liking FNR to a viologen molecule (which as a single electron carrier would generate a semiquinone at the FAD) converts the enzyme to an efficient NADPH oxidase (Bes et al., 1995). The ratio of PSI:Fd:FNR therefore seems critical to minimize $O_2^{\bullet-}$ production during PET.

Interestingly, a spin trapping study on $O_2^{\bullet-}$ generation by chloroplasts found that the *trol* mutant, which lacks an FNR-membrane tether and has decreased FNR at the membrane, also shows decreased $O_2^{\bullet-}$ evolution (Vojta et al., 2015). As this difference is also seen on addition of MV, it is presumably unrelated to the photoreduction of FNR via Fd that we have measured with isolated thylakoids. Rather, the use of intact chloroplasts by Vojta et al. (2015) with theoretically intact ROS-quenching mechanisms indicates that an alternative quenching mechanism might be responsible.

FNR Mutants and Overexpressors Both Show Gene Expression Responses Associated with Oxidative Stress under Ambient Conditions

Increased $O_2^{\bullet-}$ on perturbation of FNR content should be detectable at the level of gene expression, where many ROS markers have been identified (Mehta et al., 1992; Wagner et al., 2004). We selected markers for general

oxidative stress, $O_2^{\bullet-}$-specific stress (*At2g21640* and *DIR5*, respectively), and genes potentially up-regulated in response to both *FNR* loss and ROS or redox perturbation (Supplemental Table S2). Expression of the *WRKY70* transcription factor is induced by ROS (Brosché et al., 2014) and red light (Joo et al., 2005), and the protein counteracts cell death during senescence and plant defense by inducing a salicylic acid response and suppressing a jasmonic acid response (Li et al., 2004, 2006; Ulker et al., 2007; Shim et al., 2013). *WRKY53* is highly induced by H_2O_2 and acts antagonistically to WRKY70, accelerating cell death during senescence and defense (Besseau et al., 2012). *SAG21* is another senescence-associated gene whose expression is triggered by H_2O_2 and $O_2^{\bullet-}$ (Salleh et al., 2012) and is reported to confer tolerance to oxidative stress in yeast (Mowla et al., 2006). *ACD6* and *SYP122* are additional components of the salicylic acid-signaling network initiated during defense (Lu et al., 2003; Zhang et al., 2007, 2008; Tateda et al., 2015). Interestingly, both *WRKY53* and *SAG21* were also found to be up-regulated in *trol* mutants (Jurić et al., 2009). Unexpectedly, qRT-PCR indicates that mRNAs of these genes are increased not only in *fnr1* but also in both Zm*FNR1*- and Zm*FNR3*-expressing plants, which additionally show up-regulation of oxidative stress and $O_2^{\bullet-}$-specific markers (Fig. 6). This finding opens up the intriguing possibility that the protection against oxidative stress in FNR overexpressing plants might be partly due to systemic acquired acclimation (Rao et al., 1997), with plants "primed" by $O_2^{\bullet-}$ generated under growth-light conditions preinducing oxidative stress protection. This may partly explain their increased tolerance to high-light stress (Fig. 7). Critically, although *fnr1* plants do show increased expression of some genes that respond to oxidative stress, the specific marker for $O_2^{\bullet-}$ is not up-regulated (Fig. 6), consistent with a lack of priming and a failure to increase high-light tolerance (Fig. 7).

Relative Contributions of Membrane-Bound and Soluble FNR

In vitro measurements allowed us to dissect the impact of increased membrane-bound FNR, which results in lower $O_2^{\bullet-}$ production (Fig. 4C) from increased soluble FNR, which resulted in increased $O_2^{\bullet-}$ production (Fig. 5). However, expression of both membrane-bound and soluble FNR resulted in perception of $O_2^{\bullet-}$ at the level of gene expression (Fig. 6) and improved high-light tolerance (Fig. 7). All FNR-expressing lines also contain native FNR in both soluble and membrane-bound locations, and so the results indicate that total FNR content may be more critical than localization under these growth conditions. However, plants expressing membrane-bound FNR have a more reduced glutathione pool (Fig. 3) and were slightly more tolerant to high-light stress than those expressing soluble FNR (Fig. 7). In combination with the observation that *fnr2* plants (which have membrane-bound FNR) are more stress tolerant than *fnr1* plants (which have only soluble FNR) at low temperature (Lintala et al., 2009), this supports a greater role for membrane-bound FNR in stress tolerance.

Metabolic Impact of FNR on Redox Poise and Stress Tolerance

FNR contents, in particular of membrane-bound FNR, correlate with glutathione redox poise (Fig. 3) and activation state of the NADP-MDH, which is a readout of $NADP^+$/NADPH redox poise (Fig. 2). Based on these data, we propose that the velocity of NADPH regeneration may be translated to the redox poise of chloroplast glutathione. This has previously been reported for the cytosol, where inhibition of the oxidative pentose phosphate pathway prevents $NADP^+$ reduction, resulting in a more oxidized glutathione pool (Mou et al., 2003). However, the changes in glutathione redox poise seen in Figure 3 are unlikely to result in altered ascorbate regeneration, because the ascorbate: dehydroascorbate reductase redox couple has a much more positive redox potential than the GSH/GSSG redox couple (Foyer and Noctor, 2011) and will therefore remain predominantly reduced even when the majority of glutathione is oxidized. For this reason, differences in ascorbate regeneration can probably be discounted as the cause of altered stress tolerance of *fnr1* and Zm*FNR1* plants (Fig. 7). Alternatively, altered glutathione redox poise in *fnr1* and Zm*FNR* lines might influence signaling cascades originating in cytosolic glutathione (Chen and Dickman, 2004; Mhamdi et al., 2010). Oxidized cytosolic glutathione can be transported into the vacuole (Queval et al., 2011) and the chloroplast membrane contains glutathione transporters (Maughan et al., 2010), suggesting that chloroplast glutathione redox poise might also be transmitted to the cytosol. Indeed, WRKY53 has been shown to interact with a GST in a yeast 2-hybrid screen (Van Eck et al., 2014), providing a link between glutathione redox poise and genes with increased transcript in both *fnr1* and Zm*FNR* lines (Fig. 6).

Finally, altered FNR activity might also impact on the metabolic capacity of the cell to dissipate oxidative stress. For example, disturbed NADPH/$NADP^+$ ratios could result in altered electron supply, not only to GR, but also other NADPH-dependent enzymes involved in stress response such as chloroplast alkenal/one oxidoreductase (Yamauchi et al., 2012). As highlighted in Figure 1, chloroplast stress relief enzymes are supported by both Fd and NADPH reduction systems. The correlation between FNR content and stress tolerance might reflect the capacity to interconvert Fd and NADPH, allowing the plant to rapidly exploit both Fd- and NADPH-dependent ROS removal and regulatory mechanisms in the chloroplast (Asada, 1999; Hanke et al., 2009; Foyer and Noctor, 2011).

In summary, our work indicates that the ratio between components at the end of the linear electron transport chain is critical to efficiently couple the Fd/Fd^{red} and $NADP^+$/NADPH redox pools, prevent superoxide generation, and balance the chloroplast redox

poise. The resultant disturbances in chloroplast and glutathione redox poise and in ROS perception will influence the plant's investment in either photosynthetic apparatus or stress response machinery and therefore affect growth efficiency. This provides an example of how fine-tuning the ratio of specific PET chain components can induce a stress acclimation response.

METHODS

Plant Growth, Chloroplast Isolation, and Thylakoid Preparation

Unless otherwise indicated, plants were grown in 10 h light at 21°C, 14 h dark at 18°C. Chloroplast preparation for electron transport and EPR measurements with thylakoid membranes was basically as described previously (Hanke et al., 2008). Genotypes wild-type Col and *fnr1* were as described previously (Hanke et al., 2008), and maize *FNR1*- and *FNR3*-overexpressing plants were as described previously (Twachtmann et al., 2012). Plants for high-light treatment were germinated under Lumilux cool-white lights (Osram FQ) at 150 μE s^{-1} m^{-2} and transferred to growth chambers with SON-T Agro lamps (Phillips, Eindhoven, The Netherlands) at the same light intensity 1 week before high-light treatment at 600 μE s^{-1} m^{-2} under SON-T Agro lamps.

Measurements of Electron Transfer Activity in Isolated Thylakoids

Total electron transfer capacity of thylakoids was measured as electron flux to $[Fe(CN)_6]^{3-}$ on illumination with light >610 nm (cutoff filter) at 600 μE m^{-2} s^{-1} in a 1-mm light path cuvette. Reactions contained thylakoids at a final chlorophyll concentration of 33 μg mL^{-1}, 330 mM sorbitol, 50 mM HEPES, 20 mM NaCl, 5 mM $MgCl_2$, 0.1 μM nigericin, and 500 μM $[Fe(CN)_6]^{3-}$. Absorbance difference between 420 and 540 nm was measured after 0, 0.5, 1, 2, and 5 min illumination to calculate the rate. $NADP^+$ photoreduction was measured in an identical system, substituting 5 μM Arabidopsis (*Arabidopsis thaliana*) Fd2 and 200 μM $NADP^+$ for $[Fe(CN)_6]^{3-}$ and following the change in absorbance difference between 340 and 390 nm. Total FNR activity was measured in the supernatant following a 0.1% Triton X-100 wash of thylakoid membranes to remove all peripheral proteins. The reaction was followed in a cytochrome *c* reduction assay as described previously (Hanke et al., 2004) in the presence of a 10-μM concentration of Arabidopsis Fd2 (purified as described by Hanke et al., 2004).

Determination of NADP-MDH Activation State

Measurements were performed basically as described previously (Scheibe and Stitt, 1988). In brief, leaf material was rapidly sandwiched between two sheets of solid CO_2 before grinding in liquid nitrogen, avoiding any shading prior to freeze-clamp. All following steps were performed in degassed buffers under N_2. Protein was extracted into 50 mM HEPES, pH 6, 2 mM EDTA, 2 mM dithiothreitol, 1 mM Pefabloc, 0.1% bovine serum albumin (BSA), and 0.1% Triton X-100 to maintain in situ activity, and enzyme activity was measured in 100 mM Tris-HCl, pH 8, 1 mM EDTA, 0.1% BSA, 0.2 mM NADPH. Reactions were started by addition of 1 mM oxaloacetic acid, and rates were followed at 340 nm. Rates were corrected for nonspecific NADP-dependent activity of the more abundant NAD-MDH (0.2% of the NAD-dependent rate was assumed to be due to the nonspecific NADP-dependent activity; NAD-MDH activity was measured at a higher extract dilution by addition of NADH rather than NADPH; Scheibe and Stitt, 1988). Total activity was established by enzyme activation at room temperature in activation buffer: 200 mM Tris-HCl, pH 8.4, 1 mM EDTA, 1 mM Pefabloc, 1% BSA, 100 mM dithioerythritol. Activity was measured at 0, 10, 20, and 40 min to confirm a plateau of maximum activity.

Total and GSSG Measurements

Metabolite assays were performed on mature leaf tissue from 6- to 8-week-old plants. Tissue was always harvested under growth lights by grinding in liquid nitrogen. The assays for total and oxidized glutathione were performed with the glutathione (total) detection kit from Enzo Life Sciences (Lörrach, Germany) according to the manufacturer's instructions, except for measurement of GSSG, where 20 mM 2-vinylpyridine rather than 4-vinylpyridine was used to block free thiol sites.

EPR Spectroscopy for Superoxide Detection

Reactions were assembled at low light (<1 μE s^{-1} m^{-2}) in a quartz cuvette in a volume of 150 μL containing thylakoids (33 μg chlorophyll mL^{-1}), 330 mM sorbitol, 50 mM HEPES-NaOH, pH 7.5, 1 mM $MgCl_2$, 50 μM deferoxamine mesilate, 0.1 μM nigericin, and 3.3 μM 1-hydroxy-4-isobutyramido-2,2,6,6-tetramethylpiperidinium (Kozuleva et al., 2011) unless otherwise specified. Aliquots of 20 μL were taken for the EPR measurements. Light treatments were at 600 μE s^{-1} m^{-2} for 2 min at 21°C using a 100-W halogen lamp unless otherwise stated. To prevent unwanted radical formation from the spin trap by UV radiation, a cutoff filter removing wavelengths <610 nm was used. EPR measurements were performed at room temperature (296–299 K) with a homemade X-band EPR spectrometer equipped with a Bruker dielectric resonator or on a Miniscope X-band benchtop EPR spectrometer (MS200; Magnettech GmbH, Berlin, Germany) equipped with a rectangular TE102 resonator, with the microwave power set to 0.4 to 0.6 mW and B-field modulation amplitude adjusted to 0.15 mT. Samples were measured in EPR glass capillaries (0.9 mm i.d.).

The $O_2^{\bullet-}$ radical concentration was calculated using a standard solution of the stable nitroxide radical TEMPOL at a known concentration. To distinguish soluble $O_2^{\bullet-}$ generation from radical production within the thylakoid membrane, SOD (200 U mL^{-1}) was added to the suspension. The total rate of $O_2^{\bullet-}$ generation was equal to the rate of nitroxide radical accumulation in the absence of SOD. The rate of soluble ("stromal") $O_2^{\bullet-}$ generation was calculated by subtracting the rate of nitroxide radical accumulation in the presence of SOD (+SOD) from the total rate (−SOD).

Recombinant maize FNR3 was prepared as described previously (Okutani et al., 2005).

qRT-PCR

Total RNA was isolated from 100 mg frozen leaf material by using PureLink RNA Mini Kit (Ambion, Thermo Fisher Scientific, Darmstadt, Germany) as per the manufacturer's protocol, with some additional modifications. After RNA isolation, DNase digestion was performed to remove genomic DNA using TURBO DNA-free Kit (Ambion, Thermo Fisher Scientific). The method was performed according to the manufacturer's instructions. After RNA isolation and DNase treatment, samples were analyzed by qPCR to test for contamination with genomic DNA using intron-specific primers (Supplemental Table S3). Afterward, cDNA was synthesized from 2 μg total RNA using oligo(dT) as primers according to the manufacturer's instructions (Fermentas RevertAid First Strand cDNA Synthesis Kit, Fermentas GmbH, St. Leon-Rot, Germany).

qRT-PCR was performed as described previously (Karpinski et al., 1999). Briefly, all primers were tested for their precise annealing temperature and efficiency before use. A PCR assay efficiency range from 90% to 110% was considered acceptable. Thereafter, only primers exhibiting this efficiency were used and are shown in Supplemental Table S3. Real-time PCR was performed using a Thermal Cycler (C1000, Biorad, München) and a real-time system (CFX96, Biorad, München). All transcripts were normalized to the housekeeping gene *RAN3*.

Chlorophyll Fluorescence and Membrane Leakage

Measurements were performed on 1-cm diameter leaf discs cut from mature leaves of 6- to 8-week-old plants. Leaf discs were floated on 4 mL MilliQ water before high-light treatment. Ion leakage was detected as conductivity of the water solution measured with an electrode (Hannah Instruments, Kehl am Rhein, Germany), and fluorescence of leaf discs was measured using a FluorCam (Photon Systems Instruments, Brno, Czech Republic). PSII capacity was calculated following 10 min dark adaptation, as F_V (variable fluorescence after dark adaptation)/F_M (maximal fluorescence after dark adaptation).

Accession Numbers

Sequence data from this article can be found in the Arabidopsis Genome Initiative or GenBank/EMBL databases under the following accession numbers: maize FNR1, BAA88236; FNR3, ACF85815; Arabidopsis FNR1, AT5G66190; FNR2, AT1G20020; WRKY53, AT4G23810; WRKY70, AT3G56400; LEA5/SAG21, AT4G02380; ACD6, AT4G14400; SYP122, AT3G52400; RAN3, AT5G55190.

Supplemental Data

The following supplemental materials are available.

Supplemental Figure S1. Response of Arabidopsis plants with different FNR contents to high-light treatment (original data).

Supplemental Table S1. Rates of NADP-MDH activity in crude protein extracts of Arabidopsis leaves.

Supplemental Table S2. Rationale for the selection of genes investigated by qRT-PCR in Figure 6.

Supplemental Table S3. Primers used in cDNA quality control and qRT-PCR.

Received July 11, 2016; accepted September 13, 2016; published September 15, 2016.

LITERATURE CITED

Allen JF, Hall DO (1974) The relationship of oxygen uptake to electron transport in photosystem I of isolated chloroplasts: the role of superoxide and ascorbate. Biochem Biophys Res Commun **58:** 579–585

Alte F, Stengel A, Benz JP, Petersen E, Soll J, Groll M, Bölter B (2010) Ferredoxin:NADPH oxidoreductase is recruited to thylakoids by binding to a polyproline type II helix in a pH-dependent manner. Proc Natl Acad Sci USA **107:** 19260–19265

Andersen B, Scheller HV, Møller BL (1992) The PSI-E subunit of photosystem I binds ferredoxin:NADP+ oxidoreductase. FEBS Lett **311:** 169–173

Asada K (1999) The water-water cycle in chloroplasts: scavenging of active oxygens and dissipation of excess photons. Annu Rev Plant Physiol Plant Mol Biol **50:** 601–639

Backhausen JE, Kitzmann C, Scheibe R (1994) Competition between electron acceptors in photosynthesis: Regulation of the malate valve during CO2 fixation and nitrite reduction. Photosynth Res **42:** 75–86

Batie CJ, Kamin H (1981) The relation of pH and oxidation-reduction potential to the association state of the ferredoxin. ferredoxin:NADP+ reductase complex. J Biol Chem **256:** 7756–7763

Batie CJ, Kamin H (1984) Electron transfer by ferredoxin:NADP+ reductase. Rapid-reaction evidence for participation of a ternary complex. J Biol Chem **259:** 11976–11985

Batie CJ, Kamin H (1986) Association of ferredoxin-NADP+ reductase with NADP(H) specificity and oxidation-reduction properties. J Biol Chem **261:** 11214–11223

Becker B, Holtgrefe S, Jung S, Wunrau C, Kandlbinder A, Baier M, Dietz KJ, Backhausen JE, Scheibe R (2006) Influence of the photoperiod on redox regulation and stress responses in Arabidopsis thaliana L. (Heynh.) plants under long- and short-day conditions. Planta **224:** 380–393

Bes MT, De Lacey AL, Peleato ML, Fernandez VM, Gómez-Moreno C (1995) The covalent linkage of a viologen to a flavoprotein reductase transforms it into an oxidase. Eur J Biochem **233:** 593–599

Benz JP, Stengel A, Lintala M, Lee YH, Weber A, Philippar K, Gügel IL, Kaieda S, Ikegami T, Mulo P, et al (2009) Arabidopsis Tic62 and ferredoxin-NADP(H) oxidoreductase form light-regulated complexes that are integrated into the chloroplast redox poise. Plant Cell **21:** 3965–3983

Besseau S, Li J, Palva ET (2012) WRKY54 and WRKY70 co-operate as negative regulators of leaf senescence in Arabidopsis thaliana. J Exp Bot **63:** 2667–2679

Böhme H (1978) Quantitative determination of ferredoxin, ferredoxin-NADP+ reductase and plastocyanin in spinach chloroplasts. Eur J Biochem **83:** 137–141

Brosché M, Blomster T, Salojärvi J, Cui F, Sipari N, Leppälä J, Lamminmäki A, Tomai G, Narayanasamy S, Reddy RA, et al (2014) Transcriptomics and functional genomics of ROS-induced cell death regulation by RADICAL-INDUCED CELL DEATH1. PLoS Genet **10:** e1004112

Carrillo N, Ceccarelli EA (2003) Open questions in ferredoxin-NADP+ reductase catalytic mechanism. Eur J Biochem **270:** 1900–1915

Cassan N, Lagoutte B, Sétif P (2005) Ferredoxin-NADP+ reductase. Kinetics of electron transfer, transient intermediates, and catalytic activities studied by flash-absorption spectroscopy with isolated photosystem I and ferredoxin. J Biol Chem **280:** 25960–25972

Chen S, Dickman MB (2004) Bcl-2 family members localize to tobacco chloroplasts and inhibit programmed cell death induced by chloroplast-targeted herbicides. J Exp Bot **55:** 2617–2623

Chew O, Whelan J, Millar AH (2003) Molecular definition of the ascorbate-glutathione cycle in Arabidopsis mitochondria reveals dual targeting of antioxidant defenses in plants. J Biol Chem **278:** 46869–46877

Dietz KJ, Horling F, König J, Baier M (2002) The function of the chloroplast 2-cysteine peroxiredoxin in peroxide detoxification and its regulation. J Exp Bot **53:** 1321–1329

Foyer CH, Halliwell B (1976) The presence of glutathione and glutathione reductase in chloroplasts: a proposed role in ascorbic acid metabolism. Planta **133:** 21–25

Foyer CH, Noctor G (2011) Ascorbate and glutathione: the heart of the redox hub. Plant Physiol **155:** 2–18

Giró M, Carrillo N, Krapp AR (2006) Glucose-6-phosphate dehydrogenase and ferredoxin-NADP(H) reductase contribute to damage repair during the soxRS response of Escherichia coli. Microbiology **152:** 1119–1128

Goetze DC, Carpentier R (1993) Ferredoxin-NADP+ reductase is the site of oxygen reduction in pseudocyclic electron transport. Can J Bot **72:** 256–260

Groden D, Beck E (1979) H2O2 destruction by ascorbate-dependent systems from chloroplasts. Biochim Biophys Acta **546:** 426–435

Hajirezaei MR, Peisker M, Tschiersch H, Palatnik JF, Valle EM, Carrillo N, Sonnewald U (2002) Small changes in the activity of chloroplastic NADP(+)-dependent ferredoxin oxidoreductase lead to impaired plant growth and restrict photosynthetic activity of transgenic tobacco plants. Plant J **29:** 281–293

Hameister S, Becker B, Holtgrefe S, Strodtkötter I, Linke V, Backhausen JE, Scheibe R (2007) Transcriptional regulation of NADP-dependent malate dehydrogenase: comparative genetics and identification of DNA-binding proteins. J Mol Evol **65:** 437–455

Hanke G, Mulo P (2013) Plant type ferredoxins and ferredoxin-dependent metabolism. Plant Cell Environ **36:** 1071–1084

Hanke GT, Endo T, Satoh F, Hase T (2008) Altered photosynthetic electron channelling into cyclic electron flow and nitrite assimilation in a mutant of ferredoxin:NADP(H) reductase. Plant Cell Environ **31:** 1017–1028

Hanke GT, Holtgrefe S, König N, Strodkötter I, Voss I, Scheibe R (2009) Use of transgenic plants to uncover strategies for maintenance of redox homeostasis during photosynthesis. Adv Bot Res **52:** 207–251

Hanke GT, Kimata-Ariga Y, Taniguchi I, Hase T (2004) A post genomic characterization of Arabidopsis ferredoxins. Plant Physiol **134:** 255–264

Hanke GT, Okutani S, Satomi Y, Takao T, Suzuki A, Hase T (2005) Multiple iso-proteins of FNR in Arabidopsis: evidence for different contributions to chloroplast function and nitrogen assimilation. Plant Cell Environ **28:** 1146–1157

Joo JH, Wang S, Chen JG, Jones AM, Fedoroff NV (2005) Different signaling and cell death roles of heterotrimeric G protein alpha and beta subunits in the Arabidopsis oxidative stress response to ozone. Plant Cell **17:** 957–970

Jose Quiles M, Cuello J (1998) Association of ferredoxin-NADP oxidoreductase with the chloroplastic pyridine nucleotide dehydrogenase complex in barley leaves. Plant Physiol **117:** 235–244

Jurić S, Hazler-Pilepić K, Tomasić A, Lepedus H, Jelicić B, Puthiyaveetil S, Bionda T, Vojta L, Allen JF, Schleiff E, et al (2009) Tethering of ferredoxin:NADP+ oxidoreductase to thylakoid membranes is mediated by novel chloroplast protein TROL. Plant J **60:** 783–794

Karpinski S, Reynolds H, Karpinska B, Wingsle G, Creissen G, Mullineaux P (1999) Systemic signaling and acclimation in response to excess excitation energy in Arabidopsis. Science **284:** 654–657

Kohorn BD, Lane S, Smith TA (1992) An Arabidopsis serine/threonine kinase homologue with an epidermal growth factor repeat selected in yeast for its specificity for a thylakoid membrane protein. Proc Natl Acad Sci USA **89:** 10989–10992

König J, Baier M, Horling F, Kahmann U, Harris G, Schürmann P, Dietz KJ (2002) The plant-specific function of 2-Cys peroxiredoxin-mediated detoxification of peroxides in the redox-hierarchy of photosynthetic electron flux. Proc Natl Acad Sci USA **99:** 5738–5743

Kozuleva M, Klenina I, Mysin I, Kirilyuk I, Opanasenko V, Proskuryakov I, Ivanov B (2015) Quantification of superoxide radical production in thylakoid membrane using cyclic hydroxylamines. Free Radic Biol Med **89:** 1014–1023

Kozuleva M, Klenina I, Proskuryakov I, Kirilyuk I, Ivanov B (2011) Production of superoxide in chloroplast thylakoid membranes ESR study with cyclic hydroxylamines of different lipophilicity. FEBS Lett **585:** 1067–1071

Kozuleva MA, Ivanov BN (2010) Evaluation of the participation of ferredoxin in oxygen reduction in the photosynthetic electron transport chain of isolated pea thylakoids. Photosynth Res **105:** 51–61

Kozuleva MA, Petrova AA, Mamedov MD, Semenov AY, Ivanov BN (2014) O_2 reduction by photosystem I involves phylloquinone under steady-state illumination. FEBS Lett **588:** 4364–4368

Krapp AR, Rodriguez RE, Poli HO, Paladini DH, Palatnik JF, Carrillo N (2002) The flavoenzyme ferredoxin (flavodoxin)-NADP(H) reductase modulates NADP(H) homeostasis during the soxRS response of Escherichia coli. J Bacteriol **184:** 1474–1480

Krapp AR, Tognetti VB, Carrillo N, Acevedo A (1997) The role of ferredoxin-NADP+ reductase in the concerted cell defense against oxidative damage: studies using Escherichia coli mutants and cloned plant genes. Eur J Biochem **249:** 556–563

Krieger-Liszkay A, Fufezan C, Trebst A (2008) Singlet oxygen production in photosystem II and related protection mechanism. Photosynth Res **98:** 551–564

Krieger-Liszkay A, Kós PB, Hideg E (2011) Superoxide anion radicals generated by methylviologen in photosystem I damage photosystem II. Physiol Plant **142:** 17–25

Li J, Brader G, Kariola T, Palva ET (2006) WRKY70 modulates the selection of signaling pathways in plant defense. Plant J **46:** 477–491

Li J, Brader G, Palva ET (2004) The WRKY70 transcription factor: a node of convergence for jasmonate-mediated and salicylate-mediated signals in plant defense. Plant Cell **16:** 319–331

Lintala M, Allahverdiyeva Y, Kangasjärvi S, Lehtimäki N, Keränen M, Rintamäki E, Aro EM, Mulo P (2009) Comparative analysis of leaf-type ferredoxin-NADP oxidoreductase isoforms in Arabidopsis thaliana. Plant J **57:** 1103–1115

Lintala M, Allahverdiyeva Y, Kidron H, Piippo M, Battchikova N, Suorsa M, Rintamäki E, Salminen TA, Aro EM, Mulo P (2007) Structural and functional characterization of ferredoxin-NADP+-oxidoreductase using knock-out mutants of Arabidopsis. Plant J **49:** 1041–1052

Lintala M, Lehtimäki N, Benz JP, Jungfer A, Soll J, Aro EM, Bölter B, Mulo P (2012) Depletion of leaf-type ferredoxin-NADP(+) oxidoreductase results in the permanent induction of photoprotective mechanisms in Arabidopsis chloroplasts. Plant J **70:** 809–817

Lintala M, Schuck N, Thormählen I, Jungfer A, Weber KL, Weber AP, Geigenberger P, Soll J, Bölter B, Mulo P (2014) Arabidopsis tic62 trol mutant lacking thylakoid-bound ferredoxin-NADP+ oxidoreductase shows distinct metabolic phenotype. Mol Plant **7:** 45–57

Liochev SI, Hausladen A, Beyer WF Jr, Fridovich I (1994) NADPH: ferredoxin oxidoreductase acts as a paraquat diaphorase and is a member of the soxRS regulon. Proc Natl Acad Sci USA **91:** 1328–1331

Liu J, Wang P, Liu B, Feng D, Zhang J, Su J, Zhang Y, Wang JF, Wang HB (2013) A deficiency in chloroplastic ferredoxin 2 facilitates effective photosynthetic capacity during long-term high light acclimation in Arabidopsis thaliana. Plant J **76:** 861–874

Lu H, Rate DN, Song JT, Greenberg JT (2003) ACD6, a novel ankyrin protein, is a regulator and an effector of salicylic acid signaling in the Arabidopsis defense response. Plant Cell **15:** 2408–2420

Martínez-Júlvez M, Medina M, Velázquez-Campoy A (2009) Binding thermodynamics of ferredoxin:NADP+ reductase: two different protein substrates and one energetics. Biophys J **96:** 4966–4975

Maughan SC, Pasternak M, Cairns N, Kiddle G, Brach T, Jarvis R, Haas F, Nieuwland J, Lim B, Müller C, et al (2010) Plant homologs of the Plasmodium falciparum chloroquine-resistance transporter, PfCRT, are required for glutathione homeostasis and stress responses. Proc Natl Acad Sci USA **107:** 2331–2336

Mehta RA, Fawcett TW, Porath D, Mattoo AK (1992) Oxidative stress causes rapid membrane translocation and in vivo degradation of ribulose-1,5-bisphosphate carboxylase/oxygenase. J Biol Chem **267:** 2810–2816

Mehterov N, Balazadeh S, Hille J, Toneva V, Mueller-Roeber B, Gechev T (2012) Oxidative stress provokes distinct transcriptional responses in the stress-tolerant atr7 and stress-sensitive loh2 Arabidopsis thaliana mutants as revealed by multi-parallel quantitative real-time PCR analysis of ROS marker and antioxidant genes. Plant Physiol Biochem **59:** 20–29

Mhamdi A, Hager J, Chaouch S, Queval G, Han Y, Taconnat L, Saindrenan P, Gouia H, Issakidis-Bourguet E, Renou JP, et al (2010) Arabidopsis GLUTATHIONE REDUCTASE1 plays a crucial role in leaf responses to intracellular hydrogen peroxide and in ensuring appropriate gene expression through both salicylic acid and jasmonic acid signaling pathways. Plant Physiol **153:** 1144–1160

Misra HP, Fridovich I (1971) The generation of superoixide radical during the autoxidation of ferredoxins. J Biol Chem **246:** 6886–6890

Mittler R, Vanderauwera S, Gollery M, Van Breusegem F (2004) Reactive oxygen gene network of plants. Trends Plant Sci **9:** 490–498

Miyake C, Schreiber U, Hormann H, Sano S, Asada K (1998) The FAD-enzyme monodehydroascorbate radical reductase mediates photoproduction of superoxide radicals in spinach thylakoid membranes. Plant Cell Physiol **39:** 821–829

Mou Z, Fan W, Dong X (2003) Inducers of plant systemic acquired resistance regulate NPR1 function through redox changes. Cell **113:** 935–944

Mowla SB, Cuypers A, Driscoll SP, Kiddle G, Thomson J, Foyer CH, Theodoulou FL (2006) Yeast complementation reveals a role for an Arabidopsis thaliana late embryogenesis abundant (LEA)-like protein in oxidative stress tolerance. Plant J **48:** 743–756

Mubarakshina MM, Ivanov BN (2010) The production and scavenging of reactive oxygen species in the plastoquinone pool of chloroplast thylakoid membranes. Physiol Plant **140:** 103–110

Mubarakshina Borisova MM, Kozuleva MA, Rudenko NN, Naydov IA, Klenina IB, Ivanov BN (2012) Photosynthetic electron flow to oxygen and diffusion of hydrogen peroxide through the chloroplast envelope via aquaporins. Biochim Biophys Acta **1817:** 1314–1321

Oelze ML, Kandlbinder A, Dietz KJ (2008) Redox regulation and overreduction control in the photosynthesizing cell: complexity in redox regulatory networks. Biochim Biophys Acta **1780:** 1261–1272

Okutani S, Hanke GT, Satomi Y, Takao T, Kurisu G, Suzuki A, Hase T (2005) Three maize leaf ferredoxin:NADPH oxidoreductases vary in subchloroplast location, expression, and interaction with ferredoxin. Plant Physiol **139:** 1451–1459

Palatnik JF, Tognetti VB, Poli HO, Rodríguez RE, Blanco N, Gattuso M, Hajirezaei MR, Sonnewald U, Valle EM, Carrillo N (2003) Transgenic tobacco plants expressing antisense ferredoxin-NADP(H) reductase transcripts display increased susceptibility to photo-oxidative damage. Plant J **35:** 332–341

Palatnik JF, Valle EM, Carrillo N (1997) Oxidative stress causes ferredoxin-NADP+ reductase solubilization from the thylakoid membranes in methyl viologen-treated plants. Plant Physiol **115:** 1721–1727

Pulido P, Spínola MC, Kirchsteiger K, Guinea M, Pascual MB, Sahrawy M, Sandalio LM, Dietz KJ, González M, Cejudo FJ (2010) Functional analysis of the pathways for 2-Cys peroxiredoxin reduction in Arabidopsis thaliana chloroplasts. J Exp Bot **61:** 4043–4054

Queval G, Jaillard D, Zechmann B, Noctor G (2011) Increased intracellular H_2O_2 availability preferentially drives glutathione accumulation in vacuoles and chloroplasts. Plant Cell Environ **34:** 21–32

Rao MV, Paliyath G, Ormrod DP, Murr DP, Watkins CB (1997) Influence of salicylic acid on H2O2 production, oxidative stress, and H2O2-metabolizing enzymes. Salicylic acid-mediated oxidative damage requires H2O2. Plant Physiol **115:** 137–149

Rodriguez RE, Lodeyro A, Poli HO, Zurbriggen M, Peisker M, Palatnik JF, Tognetti VB, Tschiersch H, Hajirezaei MR, Valle EM, et al (2007) Transgenic tobacco plants overexpressing chloroplastic ferredoxin-NADP(H) reductase display normal rates of photosynthesis and increased tolerance to oxidative stress. Plant Physiol **143:** 639–649

Salleh FM, Evans K, Goodall B, Machin H, Mowla SB, Mur LA, Runions J, Theodoulou FL, Foyer CH, Rogers HJ (2012) A novel function for a redox-related LEA protein (SAG21/AtLEA5) in root development and biotic stress responses. Plant Cell Environ **35:** 418–429

Scheibe R (2004) Malate valves to balance cellular energy supply. Physiol Plant **120:** 21–26

Scheibe R, Backhausen JE, Emmerlich V, Holtgrefe S (2005) Strategies to maintain redox homeostasis during photosynthesis under changing conditions. J Exp Bot **56:** 1481–1489

Scheibe R, Dietz KJ (2012) Reduction-oxidation network for flexible adjustment of cellular metabolism in photoautotrophic cells. Plant Cell Environ **35:** 202–216

Scheibe R, Stitt M (1988) Comparison of NADP-malate dehydrogenase activation, QA reduction and O2 evolution in spinach leaves. Plant Physiol Biochem **26:** 473–481

Schürmann P, Buchanan BB (2008) The ferredoxin/thioredoxin system of oxygenic photosynthesis. Antioxid Redox Signal **10:** 1235–1274

Shim JS, Jung C, Lee S, Min K, Lee YW, Choi Y, Lee JS, Song JT, Kim JK, Choi YD (2013) AtMYB44 regulates WRKY70 expression and modulates antagonistic interaction between salicylic acid and jasmonic acid signaling. Plant J **73:** 483–495

Snyrychová I, Pospísil P, Naus J (2006) Reaction pathways involved in the production of hydroxyl radicals in thylakoid membrane: EPR spin-trapping study. Photochem Photobiol Sci **5:** 472–476

Tateda C, Zhang Z, Greenberg JT (2015) Linking pattern recognition and salicylic acid responses in Arabidopsis through ACCELERATED CELL DEATH6 and receptors. Plant Signal Behav **10:** e1010912

Telfer A, Bishop SM, Phillips D, Barber J (1994) Isolated photosynthetic reaction center of photosystem II as a sensitizer for the formation of singlet oxygen. Detection and quantum yield determination using a chemical trapping technique. J Biol Chem **269:** 13244–13253

Tognetti VB, Palatnik JF, Fillat MF, Melzer M, Hajirezaei MR, Valle EM, Carrillo N (2006) Functional replacement of ferredoxin by a cyanobacterial flavodoxin in tobacco confers broad-range stress tolerance. Plant Cell **18:** 2035–2050

Twachtmann M, Altmann B, Muraki N, Voss I, Okutani S, Kurisu G, Hase T, Hanke GT (2012) N-terminal structure of maize ferredoxin: NADP+ reductase determines recruitment into different thylakoid membrane complexes. Plant Cell **24:** 2979–2991

Ulker B, Shahid Mukhtar M, Somssich IE (2007) The WRKY70 transcription factor of Arabidopsis influences both the plant senescence and defense signaling pathways. Planta **226:** 125–137

Van Eck L, Davidson RM, Wu S, Zhao BY, Botha AM, Leach JE, Lapitan NL (2014) The transcriptional network of WRKY53 in cereals links oxidative responses to biotic and abiotic stress inputs. Funct Integr Genomics **14:** 351–362

Vojta L, Carić D, Cesar V, Antunović Dunić J, Lepeduš H, Kveder M, Fulgosi H (2015) TROL-FNR interaction reveals alternative pathways of electron partitioning in photosynthesis. Sci Rep **5:** 10085

Wagner D, Przybyla D, Op den Camp R, Kim C, Landgraf F, Lee KP, Würsch M, Laloi C, Nater M, Hideg E, et al (2004) The genetic basis of singlet oxygen-induced stress responses of Arabidopsis thaliana. Science **306:** 1183–1185

Yamauchi Y, Hasegawa A, Mizutani M, Sugimoto Y (2012) Chloroplastic NADPH-dependent alkenal/one oxidoreductase contributes to the detoxification of reactive carbonyls produced under oxidative stress. FEBS Lett **586:** 1208–1213

Yang C, Hu H, Ren H, Kong Y, Lin H, Guo J, Wang L, He Y, Ding X, Grabsztunowicz M, et al (2016) LIGHT-INDUCED RICE1 regulates light-dependent attachment of LEAF-TYPE FERREDOXIN-NADP+ OXIDOREDUCTASE to the thylakoid membrane in rice and Arabidopsis. Plant Cell **28:** 712–728

Zhang H, Whitelegge JP, Cramer WA (2001) Ferredoxin:NADP+ oxidoreductase is a subunit of the chloroplast cytochrome b6f complex. J Biol Chem **276:** 38159–38165

Zhang Z, Feechan A, Pedersen C, Newman MA, Qiu JL, Olesen KL, Thordal-Christensen H (2007) A SNARE-protein has opposing functions in penetration resistance and defence signalling pathways. Plant J **49:** 302–312

Zhang Z, Lenk A, Andersson MX, Gjetting T, Pedersen C, Nielsen ME, Newman MA, Hou BH, Somerville SC, Thordal-Christensen H (2008) A lesion-mimic syntaxin double mutant in Arabidopsis reveals novel complexity of pathogen defense signaling. Mol Plant **1:** 510–527